

Signatures of a surviving helium-star companion in Type Ia supernovae and constraints on the progenitor companion of SN 2011fe

ZHENG-WEI LIU,^{1,2,3} FRIEDRICH K. RÖPKE,^{4,5} AND YAOTIAN ZENG^{1,2,3}

¹*Yunnan Observatories, Chinese Academy of Sciences (CAS), 396 Yangfangwang, Guandu District, Kunming 650216, China*

²*Key Laboratory for the Structure and Evolution of Celestial Objects, CAS, Kunming 650216, China*

³*University of Chinese Academy of Science, Beijing 100012, China*

⁴*Zentrum für Astronomie der Universität Heidelberg, Institut für Theoretische Astrophysik, Philosophenweg 12, 69120 Heidelberg, Germany*

⁵*Heidelberger Institut für Theoretische Studien, Schloss-Wolfsbrunnengasse 35, 69118 Heidelberg, Germany*

ABSTRACT

Single-degenerate (SD) binary systems composed of a white dwarf and a non-degenerate helium (He)-star companion have been proposed as the potential progenitors of Type Ia supernovae (SNe Ia). The He-star companions are expected to survive the SN Ia explosion in this SD progenitor model. In the present work, we map the surviving He-star companion models computed from our previous three-dimensional hydrodynamical simulations of ejecta-companion interaction into the one-dimensional stellar evolution code `Modules for Experiments in Stellar Astrophysics (MESA)` to follow their long-term evolution to make predictions on their post-impact observational properties, which can be helpful for searches of such surviving He-star companions in future observations. By comparing with the very late-epoch light curve of the best observed SN Ia, SN 2011fe, we find that our surviving He-star companions become significantly more luminous than SN 2011fe about 1000 d after the maximum light. This suggests that a He star is very unlikely to be a companion to the progenitor of SN 2011fe.

Keywords: Type Ia supernovae (1728) — Hydrodynamical simulations (767) — Close binary stars (254) — Stellar evolution (1599) — Helium-rich stars (715) — Companion stars (291)

1. INTRODUCTION

Type Ia supernovae (SNe Ia) have been used as cosmic distance indicators because their peak luminosities can be empirically standardized by the so-called ‘Phillips relation’ (Phillips 1993; Phillips et al. 1999), which has led to the discovery of the accelerating expansion of the Universe (Riess et al. 1998; Schmidt et al. 1998; Perlmutter et al. 1999). In addition, SNe Ia play a fundamental role in placing constraints on the equation of state of dark energy. It is generally thought that SNe Ia result from thermonuclear explosions of white dwarfs in binary systems (Hoyle & Fowler 1960). However, it is still hard to reach a consensus on the fundamental aspects of the nature of SN Ia progenitors and their actual explosion mechanism from both, the the-

oretical and observational side (e.g., Hillebrandt et al. 2013; Maoz et al. 2014; Soker 2019). Over the past decades, a range of models has been proposed to cause the explosion of white dwarfs (WDs) giving rise to SNe Ia. The main questions are how the star reaches the explosive conditions, i.e., the progenitor channel, and how the explosion proceeds, i.e., the explosion scenario. For the first, the main distinction is into the single degenerate (SD; e.g., Whelan & Iben 1973; Nomoto 1982; Hachisu et al. 1996; Han & Podsiadlowski 2004) and the double degenerate (DD; e.g., Iben & Tutukov 1984; Webbink 1984; Dan et al. 2011) channels. The explosion mechanism depends mainly on the question of whether the WD explodes near the Chandrasekhar mass (e.g., Nomoto et al. 1984; Röpke et al. 2007; Röpke & Niemeyer 2007; Seitenzahl et al. 2013; Jordan et al. 2012; Fink et al. 2014; Lach et al. 2021a,b; Livio & Riess 2003; Ilkov & Soker 2012) or at a mass below this limit (e.g., Woosley et al. 1986; Fink et al. 2007;

Shen & Bildsten 2007; Sim et al. 2010; Pakmor et al. 2010; Townsley et al. 2019; Gronow et al. 2020, 2021; Benz et al. 1989; Rosswog et al. 2009; Kushnir et al. 2013). To provide important clues on the yet poorly understood origin and explosion mechanism of SNe Ia, one needs to compare the observational features predicted by different progenitor models with the observations.

In the SD scenario, the WD accretes matter from a non-degenerate companion star through Roche-lobe overflow to trigger a thermonuclear explosion when its mass approaches the Chandrasekhar-mass limit (e.g., Whelan & Iben 1973; Han & Podsiadlowski 2004; Liu & Stancliffe 2018, 2020), in which the donor star could be either a main-sequence (MS), a slightly evolved MS, a red-giant (RG), or a helium (He) star.

On the one hand, a non-degenerate companion star is much brighter than a WD; a luminous source (i.e. the non-degenerate companion) is therefore expected to be detected in pre-explosion image at position of the SN Ia. Analyzing pre-explosion images at the SN position provides a direct way to identify the SD progenitor scenario (Foley et al. 2014; McCully et al. 2014). The pre-explosion observable properties of different non-degenerate donors at the moment of SN Ia explosion in the SD scenario have been comprehensively addressed for normal SNe Ia (Han 2008) and SNe Iax¹ (Liu et al. 2015). To date, no companion star of a normal SNe Ia has been directly confirmed in pre-explosion images (e.g. Maoz & Mannucci 2008; Li et al. 2011; Kelly et al. 2014). However, a blue luminous source has been detected in pre-explosion image of an SN Iax event, SN 2012Z (McCully et al. 2014). This pre-explosion luminous source (i.e. SN 2012Z-S1) has been interpreted as a He-star companion to the exploding WD (McCully et al. 2014; Liu et al. 2015). Interestingly, late-time observations taken about 1400 days after the explosion by the Hubble Space Telescope have shown that SN 2012Z is brighter than the normal SN 2011fe by a factor of two at this epoch (McCully et al. 2021). This excess flux is suggested to be a composite of several sources: the shock-heated companion, a bound remnant that could drive a wind, and light from the SN ejecta due to radioactive decay (McCully et al. 2021).

On the other hand, non-degenerate companion stars are expected to survive a SN Ia explosion in the SD

scenario (e.g. Wheeler et al. 1975; Marietta et al. 2000; Pakmor et al. 2008; Liu et al. 2012, 2013a,b,c, 2021; Pan et al. 2012a; Boehner et al. 2017; Bauer et al. 2019; Zeng et al. 2020). Searching for the surviving companion star in nearby SN remnants (SNRs) has been considered a promising way to test the SD progenitor scenario (e.g. Kerzendorf et al. 2009; Ruiz-Lapuente 2019). In the past few decades, many studies have been focused on searching for the surviving companion star predicted by the SD scenario in the Galactic supernova remnants (SNRs) Tycho (e.g., Ruiz-Lapuente et al. 2004; Ruiz-Lapuente 2019; Fuhrmann 2005; Ihara et al. 2007; González Hernández et al. 2009; Kerzendorf et al. 2009, 2013, 2018a; Bedin et al. 2014), Kepler (e.g., Kerzendorf et al. 2014; Ruiz-Lapuente et al. 2018), and SN 1006 (e.g., González Hernández et al. 2012; Kerzendorf et al. 2012, 2018b), and in some SNRs in the Large Magellanic Cloud (LMC): SNR 0509–67.5 (e.g., Schaefer & Pagnotta 2012; Pagnotta et al. 2014; Litke et al. 2017), SNR 0519–69.0 (e.g., Edwards et al. 2012; Li et al. 2019), SNR 0505–67.9 (DEML71, Pagnotta & Schaefer 2015), SNR 0509–68.7 (N103B, e.g., Pagnotta & Schaefer 2015; Li et al. 2017), and SNR 0548–70.4 (e.g., Li et al. 2019). To date, no surviving companion could be firmly identified in these SNRs. Shen et al. (2018) suggest that three hypervelocity runaway stars detected in *Gaia*'s second data release (Gaia Collaboration et al. 2016, 2018) are WD companions that survived so-called dynamically driven double-degenerate double-detonation ('D6') SNe Ia.

The surviving companion stars are expected to present distinct observational signatures after the explosion due to the mass-stripping, shock heating and enrichment with heavy elements from SN ejecta during the ejecta-companion interaction. Using one-dimensional (1D) stellar evolution codes, some previous studies have investigated the post-impact properties of surviving companions of SNe Ia. They followed the long-term evolution of the companion models that either were produced from three-dimensional (3D) hydrodynamical simulations of ejecta-companion interaction (e.g., Pan et al. 2012b, 2013; Liu & Zeng 2021; Liu et al. 2021) or have mimicked the interaction with the supernova ejecta by a rapid mass loss and extra heating (e.g., Podsiadlowski 2003; Shappee et al. 2013). All previous studies suggest that the surviving companion stars of SNe Ia generally become significantly more luminous after the impact during the thermal re-equilibration phase.

In our previous studies, we have performed 3D hydrodynamical simulations of ejecta-companion interaction within the He-star donor progenitor scenario of SNe Ia (Liu et al. 2013c), in which the smoothed-

¹ SNe Iax potentially form the most common subclass of SNe Ia, with an estimated rate of occurrence of about 5%–30% of the total SN Ia rate (Foley et al. 2013). Recent work suggests that weak deflagrations of a Chandrasekhar-mass WD is able to reproduce the characteristic observational features of bright SNe Iax (e.g., Jordan et al. 2012; Kromer et al. 2013; Lach et al. 2021a).

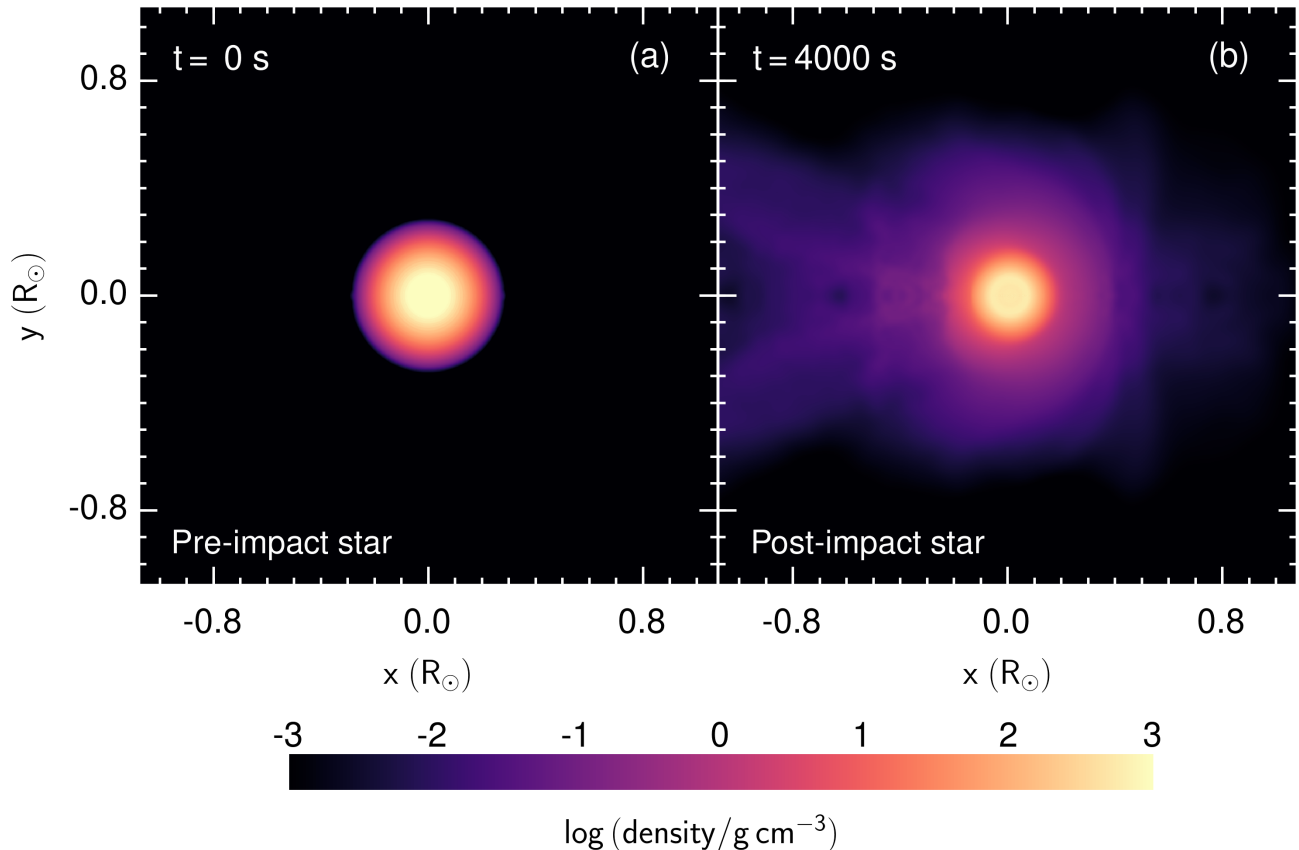


Figure 1. He-star companion at the pre-impact phase (*left panel*) and at the end of 3D hydrodynamical simulations (*right panel*) of ejecta-donor interaction in Liu et al. (2013c). The panels show density slices in the orbital plane. Here, only the so-called ‘He01’ is shown as an example. The color scale gives the logarithm of the mass density in g cm^{-3} .

particle hydrodynamics (SPH) code STELLAR GADGET (Springel et al. 2001; Pakmor et al. 2012) was adopted for our impact simulations, and a near-Chandrasekhar-mass explosion model of Nomoto et al. (1984) (i.e., the so-called W7 model) was used for representing normal SNe Ia. However, we did not address the long-term evolution and appearance of our surviving He-star companions. The main goal of this work is to provide observational properties of these surviving He-star companions by following their long-term post-impact evolution. Furthermore, we compare our results with the late-time observations of the best observed SN Ia SN 2011fe (e.g., Shappee et al. 2017; Dimitriadis et al. 2017; Kerzendorf et al. 2017) to place constraints on its progenitor model.

As mentioned above, Pan et al. (2013) also explored the long-term evolution of surviving He-star companions of SNe Ia. However, the companion models used in their 3D hydrodynamic impact simulations were constructed by artificially adopting a constant mass-loss rate instead of a detailed binary evolution calculation to mimic the

detailed binary evolutionary models. Our initial He-star companion stars (i.e., ‘He01’ and ‘He02’ model, see Table 1) were followed through the full binary evolution (Liu et al. 2013c). In model He01, the He-star companion remains in its MS phase in He01 model until the onset of the SN explosion. In model He02, in contrast, it has evolved slightly into the subgiant phase (i.e., the central He is exhausted). The detailed binary evolution (Liu et al. 2013c, see their Sect. 2) and population synthesis calculations (Wang et al. 2009, see their Figs. 3–5) suggest that these two models are likely to represent progenitors of SNe Ia. To determine observational properties for searches for surviving companions, it is important to follow the long-term evolution of our models. In addition, only few surviving companion models have been explored by previous works. An improvement to predictions on the observable features of surviving companions of SNe Ia requires further studies that cover a wider range of companion models.

2. MAPPING FROM 3D TO 1D

Table 1. Helium-star companion models and results of this work.

Name	M_2^f (M_\odot)	$\log P^f$ (days)	R_2^f (10^{10} cm)	V_{orb}^f (km s^{-1})	V_{rot}^f (km s^{-1})	$\log T_{\text{eff}}^f$ (K)	$\Delta M/M_2^f$ (%)	V_{kick} (km s^{-1})	E_{in} (10^{49} erg)	t_{peak} (yr)	L_{peak} ($10^4 L_\odot$)
He01	1.24	-1.34	1.91	432	301	4.70	2.2	66	1.68	14.94	1.65
He02	1.01	-1.12	2.48	387	237	4.85	5.6	59	1.19	29.75	0.58
He01r	1.24	-1.34	1.91	432	301	4.70	2.3	67	1.72	22.50	1.53
He02r	1.01	-1.12	2.48	387	237	4.85	5.7	60	1.19	72.36	0.44
0p8_He01r	1.24	-1.34	1.91	432	301	4.70	1.5	40	1.47	8.05	1.95
1p0_He01r	1.24	-1.34	1.91	432	301	4.70	1.9	53	1.58	15.76	1.72
1p4_He01r	1.24	-1.34	1.91	432	301	4.70	2.7	76	1.79	34.18	1.60
1p6_He01r	1.24	-1.34	1.91	432	301	4.70	3.0	86	1.88	42.24	1.45

Note. Here, the superscript letter ‘f’ means the moment of SN Ia explosion. M_2^f , P^f , R_2^f , V_{orb}^f , V_{rot}^f and $\log T_{\text{eff}}^f$ denote the final mass, orbital period, radius, orbital velocity, rotational velocity and effective temperature of the donor star, respectively; ΔM and V_{kick} are the total amount of stripped donor mass and the kick velocity received by the donor star due to the ejecta-donor interaction; E_{in} corresponds to the total amount of energy absorbed by the donor star during the interaction. ‘He01’ and ‘He02’ are two He-star companion models in Liu et al. (2013c). A suffix ‘r’ means that the orbital motion and spin of the He-star companion are included into 3D impact simulations. ‘0p8’, ‘1p0’, ‘1p4’ and ‘1p6’ mean that different kinetic energies of SN Ia ejecta of 0.8, 1.0, 1.4 and 1.6×10^{51} erg were used for 3D impact simulations (Liu et al. 2013c, see their Sec. 4.3.3).

To provide post-impact observational properties of surviving companion stars for their identifications in historical SNRs, we use the 1D stellar evolution code `Modules for Experiments in Stellar Astrophysics` (MESA; Paxton et al. 2011, 2018) to follow the post-impact evolution of these stars for a long time up to the age of historical SNRs, i.e., a few times 100–1000 yr. We use the methods described in Liu & Zeng (2021) and Liu et al. (2021) to construct suitable starting models for MESA based on 3D surviving He-star companion models (Fig. 1) computed from our previous 3D hydrodynamical impact simulations (Liu et al. 2013c). For our rotating models, we also include the angle-averaged, radial angular momentum profile derived from the SPH output when constructing the initial models for the subsequent MESA calculations. We directly apply the relaxation routines of MESA to the outcomes of 3D SPH impact simulations to obtain the 1D stellar model with a chemical, angular momentum (which is set to be zero for non-rotating models) and thermal structure that closely matches that of the 3D companion remnant model. A detailed description of the use of the relaxation routines in MESA can be found in Appendix B of Paxton et al. (2018). To test the validity of using MESA for modeling the long-term evolution of our surviving companion star models computed from 3D hydrodynamical impact simulations, we have compared the results of MESA calculations to those of the 1D hydrodynamic stellar evolution

code `Kepler` (Weaver et al. 1978; Rauscher et al. 2002; Woosley et al. 2002; Heger & Woosley 2010) in previous work (Liu et al. 2021). We find no significant difference between MESA and Kepler results for a given companion star model (Liu et al. 2021). Therefore, we only use MESA models here.

3. POST-IMPACT EVOLUTION OF SURVIVING COMPANIONS

In this section, we present the numerical results of our 1D post-impact MESA calculations for eight surviving He-star companion models (Table 1), for which the starting models – after mapping from the 3D impact simulations – have been relaxed with the routines provided in MESA. Following Pan et al. (2013), the models were ran with a fixed time-step of 10^{-8} yr for the first 10^{-6} yr. Thereafter, the time-step was automatically determined in MESA. We also explore the dependence of post-impact evolution of the surviving He-star companion on the SN Ia explosion energy and their post-impact rotation properties. The initial parameters of all models and numerical results are also summarized in Table 1.

3.1. Post-impact properties

Figure 1 shows the evolution of density in the surviving companion during our impact simulations for model ‘He01’ (Table 1). The ejecta-companion interaction removes some He-rich material from the companion’s surface and causes an energy deposition in the

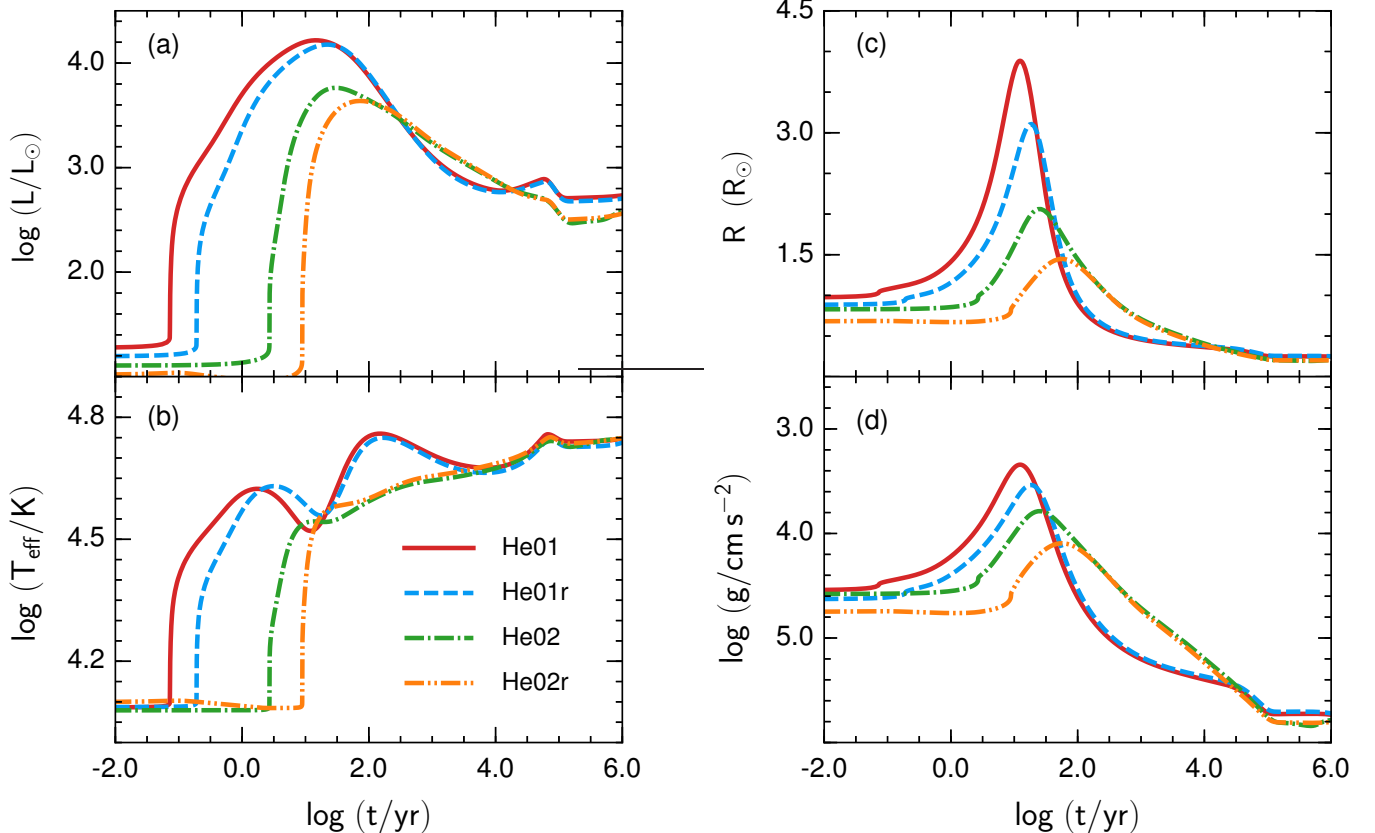


Figure 2. Post-impact evolution of the photosphere luminosity L , effective temperature T_{eff} , radius R , and surface gravity g of surviving He star companions as functions of time. The red solid and green dash-dotted curves correspond to models He01 and He02 of Liu et al. (2013c) that do not include rotation. In contrast, models He01r and He02r were set up from our 3D impact simulations including binary orbital motion and spin.

star due to the SN impact and shock heating. We find that an energy deposition of $E_{\text{in}} = 1.68 \times 10^{49}$ erg and 1.19×10^{49} erg for model He01 and He02, respectively. As a consequence, the star inflates after the explosion as shown in the right-hand panel of Fig. 1. This leads to an increase in radius by a factor of two at the end of impact simulation (about 4000 s after the explosion). Here, we use the method of Pan et al. (2013, see their Sect. 4.1) to calculate the amount of energy deposition (E_{in}) by tracing the increase of binding energy of the remnant after SN impact.

In Figure 2 we present the temporal evolution of post-impact photospheric luminosity, L (panel a), the effective temperature, T_{eff} (panel b), the radius, R (panel c), and the surface gravity, g (panel d), as functions of time for the He01 and He02 models (Table 1). The luminosities and photospheric radii of the two companion stars increase significantly as they expand. They reach peak luminosities of $L_{\text{peak}} \sim 4000\text{--}16000 L_{\odot}$ at $t_{\text{peak}} \sim 10\text{--}30$ yr after the explosion when the stars have radiated

away the deposited energy². The stars then start to contract and enter their thermal re-equilibration phase over the Kelvin-Helmholtz timescale. After re-establishing thermal equilibrium, they evolve into a B-type or O-type subdwarf (i.e., sdB or sdO) star and follow an evolutionary track of a He star with the same mass that has not experienced ejecta-companion interaction. This suggests that the details of the interaction does not significantly affect the observational properties of the surviving He-star companion of SNe Ia after they have relaxed back into thermal equilibrium. As shown in Fig. 2b, the effective temperature increases after the impact due to the reheating when the deposited energy diffuses out, although the star expands significantly at this moment. At some point, the expansion of the star becomes dominant, leading to a decrease of its effective temperature

² In this work, we define the parameters of ‘ L_{peak} ’ and ‘ t_{peak} ’ as the post-impact peak luminosity of the surviving companion star and the time of peak luminosity before the star relaxes back into the thermal equilibrium.

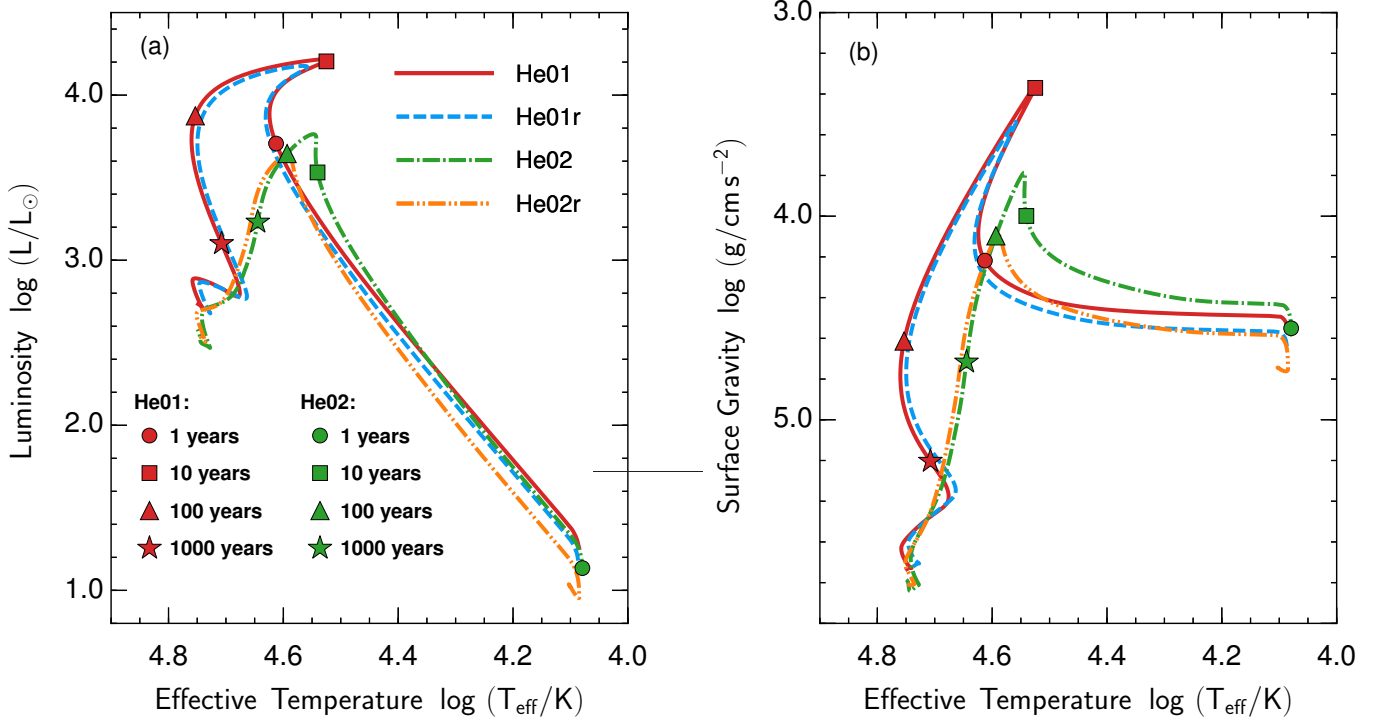


Figure 3. Post-impact evolutionary tracks of two surviving He-star companion models (i.e., He01 and He02 model of Liu et al. 2013c) in the Hertzsprung-Russell Diagram (*Left Panel*) and surface gravity vs. temperature diagram (*Right Panel*). For a comparison, the results based on the impact simulations that do include the binary orbital motion and stellar spin (i.e., the so-called ‘He01r’ and ‘He02r’ model) are given as a *blue dashes line* and *yellow double-dotted line*. The *filled circle, square, triangle, and star markers* on the tracks present post-impact evolutionary phases of 1 yr, 10 yr, 100 yr, and 1000 yr after the SN impact, respectively. Here, we have only marked different evolutionary phases of non-rotating models (i.e., the He01 and He02 model) because no significantly differences are observed in rotating models.

at about 1 yr after the explosion for He01 model. Subsequently, the effective temperature increases again as the star enters the Kelvin-Helmholtz contraction phase. Our findings are consistent with those of Pan et al. (2013). In addition, we note that the core He-burning in Model He01 and He-shell burning in Model He02 cause a small increase in the effective temperature and in the luminosity at around 10^5 yr after the impact (see left-hand side panel of Fig. 2).

Figure 3 presents evolutionary tracks of our surviving He-star companions in the Hertzsprung–Russell (H–R) diagram and in the effective temperature–surface gravity ($T_{\text{eff}}-g$) diagram. The surviving He-star companions become significantly overluminous after the impact. About a few hundred years after the explosion, the luminosity of a surviving He-star companion becomes comparable to that of a normal He-star that has not been impacted and heated. This suggests that the identification of surviving He-star companion stars of SNe Ia may be more likely to be successful for the young nearby SNRs (which should be younger than a few 100 yr).

3.2. Influence of orbital motion and stellar spin

To examine the dependence of numerical results of ejecta–companion interaction on the orbital motion and the spin of the He-star companion, Liu et al. (2013c) have carried out hydrodynamical impact simulation for He01 and He02 models by taking their orbital and spin velocities into account. Figs. 2 and 3 show how the orbital motion and the spin of the He-star companion affect the post-impact observational properties of a surviving He-star companion star. As was to be expected, we find small differences between the models that include orbital motion and spin and those that do not (Table 1). For instance, almost the same total amount of energy deposition into the companion star during the ejecta–companion interaction is observed in the rotating and non-rotating models. The post-impact peak luminosity L_{peak} and the time of peak luminosity t_{peak} change by a factor of about 1.1–1.3 and 1.5–2.4, respectively. This is in accordance with our expectations because the orbital and spin velocities (which are about 240–430 km s^{-1} , see Table 1) of a He-star companion are much lower than

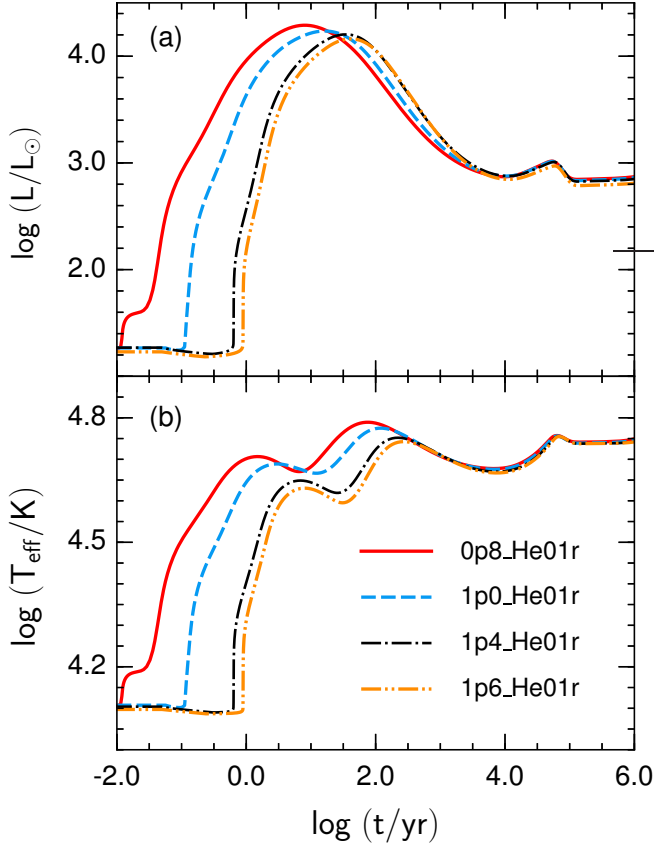


Figure 4. Similar to *left-hand panel* of Fig. 3, but for the cases artificially adopting different explosion energies (i.e., $E_{\text{kin}}^{\text{SN}} = 0.8, 1.0, 1.4$ and 1.6×10^{51} erg) in impact simulations of Liu et al. (2013c, see their Sec. 4.3.3) for the He01r model.

the typical expansion velocity of SN Ia ejecta of about 10^4 km s^{-1} .

The centrifugal force is expected to make the photosphere of the rotating model expand stronger than that of the non-rotating model and therefore the luminosity would be expected to increase faster. This, however, is not what we observe: the rise is faster and luminosities reach higher values in the non-rotating models (see Fig. 2). The reason for this counterintuitive result is that the post-impact expansion of the surviving companion star is strongly determined by the amount and depth of energy deposition. A difference between rotating and non-rotating models is seen in the depth of energy deposition into the companion star during the interaction. The depths of energy deposition (at $M_r/M_* \sim 0.98$ for the ‘He01’ model, where M_r and M_* are the enclosed mass within a sphere of radius r and the total mass of the star, respectively) are shallower in non-rotating models comparing with that of rotating models (which is at $M_r/M_* \sim 0.97$ for the ‘He01r’ model), causing

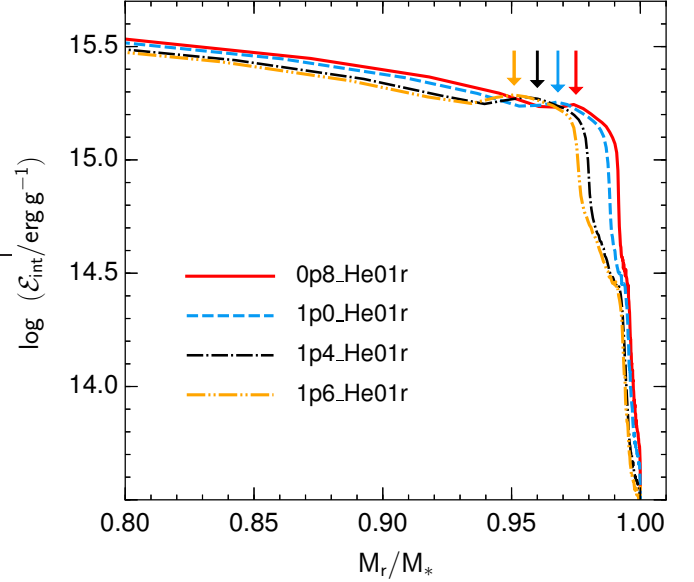


Figure 5. Specific internal energy (\mathcal{E}_{int}) of the surviving companion as a function of the mass fraction for the He01r model with different explosion energies (similar to Fig. 4). For better visibility, only the outermost layers (i.e., $M_r/M_* = 0.8-1.0$) of the star are plotted. The local maxima indicated by arrows approximately correspond to the depths of energy deposition of different cases.

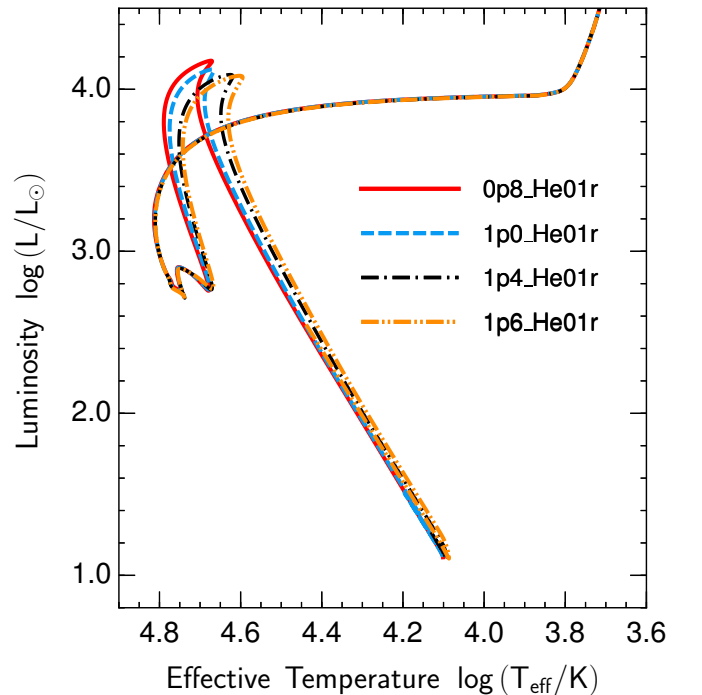


Figure 6. Similar to Fig. 3, but for the cases by artificially adopting different explosion energies in impact simulations of Liu et al. (2013c) for the He01r model.

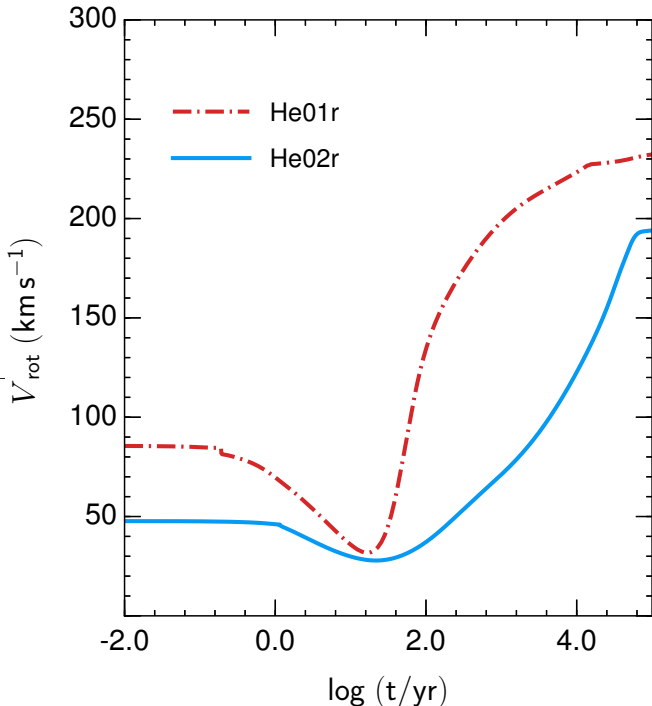


Figure 7. Similar to Fig. 2, but for the post-impact evolution of surface rotational speed of the star in model He01r (dash-dotted line) and He02r (solid line).

a shorter local radiative diffusion timescale as seen in Fig. 2. Therefore, the rotating models take longer to reach their maximum luminosities than the non-rotating models. For a given rotating model computed from our 3D impact simulation (i.e., for fixed other parameters such as amount and depth of the energy deposition), we have also done a test by following its post-impact evolution in MESA without and with including the rotation (i.e., by setting its radial angular momentum profile to be zero or not). Indeed, we find that the run including rotation has a slightly stronger expansion than the one with zero angular momentum.

3.3. Influence of the explosion energy

In Liu et al. (2013c), the typical impact simulations were ran by adopting the so-called ‘W7 model’ with an explosion energy of 1.23×10^{51} erg (Nomoto et al. 1984) to represent the SN explosion. However, the exact explosion mechanism of SNe Ia remains an open question to date. Typically, different deflagration and detonation explosion models could lead to a range of kinetic energies of the ejecta spanning 0.8 – 1.6×10^{51} erg (e.g., Röpke et al. 2007; Röpke & Niemeyer 2007; Seitenzahl et al. 2013). Therefore, Liu et al. (2013c, see their Sec. 4.3.3) artificially adjusted the kinetic energy of the SN ejecta by scaling the velocities

based on the original W7 model to investigate their effects on the ejecta-companion interaction for a given companion star model He01r (see Table 1). Here, we aim to explore the dependence of the post-impact properties of a surviving He-star companion on different kinetic energies of the supernova ejecta.

Figure 4 illustrates the post-impact luminosity and effective temperature of the surviving companion star model He01r as function of time for the cases with different SN explosion energies (i.e., kinetic energies of the ejecta of 0.8 , 1.0 , 1.4 and 1.6×10^{51} erg). An increase of the ejecta energy from 0.8×10^{51} erg (model 0p8_He01r) to 1.6×10^{51} erg (model 1p6_He01r) leads to an increase in the amount of energy deposition into the companion star increases from 1.47×10^{49} erg to 1.88×10^{49} erg (Table 1). The post-impact evolution of the surviving companion star depends strongly on the total amount and depth of energy deposition into the star during the interaction. As shown in Fig. 4, in the model with a higher kinetic energy of the ejecta (1p6_He01r) the surviving companion star reaches its peak luminosity later and has a lower peak luminosity during the early thermal re-equilibration phase. This is because the depth of energy deposition in 1p6_He01r model is deeper, although the total amount of energy deposition in this model is higher. Figure 5 shows the post-impact specific internal energy of the surviving companion star as a function of mass fraction for four cases with different kinetic energies. To better show the position of energy deposition, only the outer layers of the star (i.e., $M_r/M_* = 0.8$ – 1.0) are shown in Fig. 5. The local maximum of the internal energy seen in the envelope (i.e., the depth of energy deposition) gets deeper as the explosion energy of the ejecta increases. As a consequence, the competition between the total amount of and the depth of energy deposition leads to the results observed in Fig. 4.

Figure 6 shows post-impact evolutionary tracks of these four models in the H–R diagram. About 10^4 yr after the explosion, our four models have re-established thermal equilibrium. Subsequently, they continue to evolve on a track quite similar to that of an unperturbed He star. This suggests that different explosion energies will not significantly affect late-time evolution of the surviving companion star after its re-equilibration. Our results are consistent with those of Pan et al. (2013).

3.4. Post-impact rotation

The initial rotation of the He-star companion was set up as rigid-body rotation at the beginning of our previous 3D impact simulations Liu et al. (2013c). Under the assumption that the companion star co-rotates with its orbit due to the strong tidal interaction during the

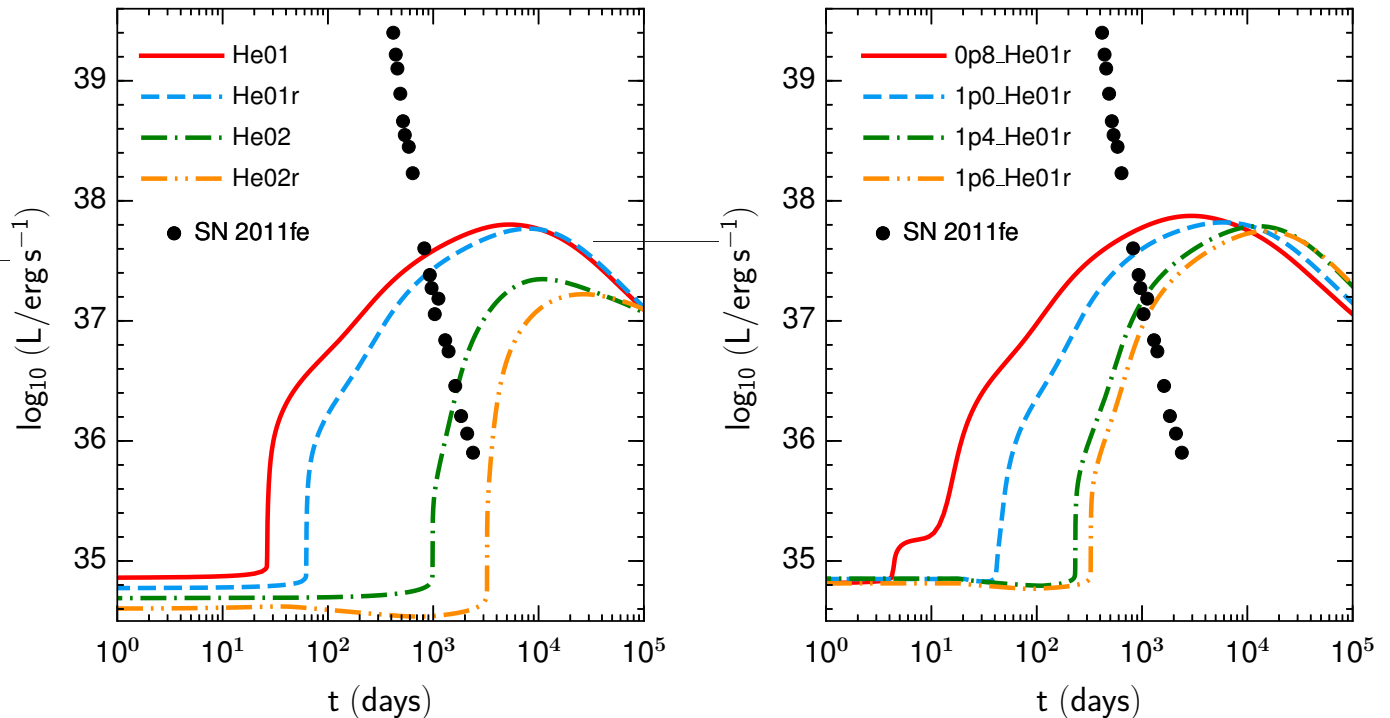


Figure 8. *Left panel:* Comparison between predicted luminosities of our surviving He-star companion models and quasi-bolometric late-time light curve (filled black circles) of SN 2011fe (e.g., Shappee et al. 2017; Kerzendorf et al. 2017; Dimitriadis et al. 2017; Tucker et al. 2021b). *Right panel:* same as left panel, but for the ‘He01r model’ with different explosion energies ($0.8, 1.0, 1.4$ and 1.6×10^{51} erg) in impact simulations (see Sect. 3.3).

pre-explosion mass-transfer phase, the companion star models He01r and He02r have rotational surface velocities as high as $V_{\text{rot}}^f = 301 \text{ km s}^{-1}$ and $V_{\text{rot}}^f = 237 \text{ km s}^{-1}$, respectively, at the onset of the SN explosion (see Table 1). After the SN impact, the He-star companions are no longer in rigid-body rotation. We find that our He01r and He02r model lose about 13% and 38%, respectively, of their initial angular momenta (Liu et al. 2013c, see their Fig. 20) as 3% and 6% of their masses are removed by the supernova blast wave. At the same time, the companion stars expand due to the shock heating. As a consequence, the surface rotational speeds in model He01r and He02r drop to $\sim 90 \text{ km s}^{-1}$ and $\sim 50 \text{ km s}^{-1}$, respectively, at the end of our impact SPH simulations.

Fig. 7 shows the post-impact evolution of the surface rotational velocities of the companions in model He01r and He02r. As expected, we find that the surface rotational velocities significantly drop as the stars expand after the impact. About 20–30 yr after the impact, when the stars reach their maximum expansion, the values decrease to about 30–40 km s^{-1} . Subsequently, the companion stars shrink, because the energy deposited by the supernova blast wave has been radiated away. This causes the surfaces to spin up again. The stars become fast-rotating objects after thermal equilibrium

is reestablished, and we find that they rotate with surface speeds of $\sim 230 \text{ km s}^{-1}$ and $\sim 190 \text{ km s}^{-1}$ in models He01r and He02r, respectively. Our results predict that the observable rotation rate of the surviving He-star companions of SNe Ia depends on the age of the SNR. Although initially the companions were fast rotators, they rotate slowly shortly after the impact of the SN blast wave and before they start to relax back into thermal equilibrium, which again leads to an increase of the rotation speed on a timescale of 10^4 yr .

4. COMPARISON WITH EXTREMELY LATE-TIME OBSERVATIONS OF SN 2011fe

SN 2011fe is one of the best-observed and closest SNe Ia (its distance is estimated with 6.4 Mpc, Shappee & Stanek 2011). This provides us with a unique opportunity to put tight constraints on the nature of its progenitor and its explosion mechanism (e.g., Nugent et al. 2011; Röpke et al. 2012; Bloom et al. 2012). Pre-explosion observations of the *Hubble Space Telescope* (HST) exclude luminous red giants ($> 3.5 M_{\odot}$) and almost all He stars as companion stars in the progenitor system of SN 2011fe (Li et al. 2011). Non-detection of early-time UV and optical emission potentially caused by shock heat-

ing in the ejecta–companion collision (Brown et al. 2012) and a lack of H-rich material in nebular spectra (e.g., Shappee et al. 2013; Graham et al. 2015; Lundqvist et al. 2015; Tucker et al. 2021a) rule out giants and MS companions. In addition, X-ray and deep radio observations disfavor most of the popular SD progenitor models (e.g., Horesh et al. 2012; Margutti et al. 2012; Chomiuk et al. 2012).

In this section, similar to that in Shappee et al. (2013), we use the extremely late-time (up to about 2400 days after the maximum light; e.g., Shappee et al. 2017; Dimitriadis et al. 2017; Kerzendorf et al. 2017; Tucker et al. 2021b) photometry observations of SN 2011fe to place further constraints on the possibility of a He-star as the companion in the progenitor system of SN 2011fe. We caution that this is meant as an example and there are reasons to believe that this supernova has not resulted from a SD progenitor system (e.g., Li et al. 2011; Nugent et al. 2011; Röpke et al. 2012; Brown et al. 2012; Horesh et al. 2012; Shappee et al. 2013). In the 3D impact simulation (Liu et al. 2013c) underlying our current study, the ‘W7 model’ of Nomoto et al. (1984) was used for representing a normal SNe Ia explosion and we therefore select the typical normal SN Ia SN 2011fe, which has the latest-epoch photometry observations so far as an example to make the comparison. Using an explosion model proposed for the ‘SNe Iax’ subclass (that is likely connected to SD progenitors) in the 3D impact simulation instead of W7, a similar comparison can be made to place constraints on the progenitor companions of sub-classes SNe Ia. Such a detailed comparison of a consistent impact model with late-time observations of a SN Iax SN 2012Z (McCully et al. 2021) will be presented in our forthcoming paper (Zeng et al. in prep).

In Figure 8, we compare the predicted luminosities of our surviving He-star companion models with the quasi-bolometric late-time light curve of SN 2011fe (Shappee et al. 2017; Dimitriadis et al. 2017; Kerzendorf et al. 2017; Tucker et al. 2021b). Our shocked He-star companion models become significantly more luminous than the observed light-curve of SN 2011fe at about 1000 d after the explosion. This means that the very late-time light curve of SN 2011fe should be more luminous than the current observations if there is indeed a shocked surviving He-star companion. This suggests that a He-star is very unlikely the mass-donating companion to the progenitor of SN 2011fe. Our conclusions are consistent with that derived from pre-explosion observations of SN 2011fe (Li et al. 2011).

As shown in Fig. 8, the latest photometry observation of SN 2011fe is still slightly luminous than our ‘He02r’ model at similar epoch, suggesting that we possibly have not yet seen a potential contribution from the shock-heated companion star with a mass of $\lesssim 0.95 M_{\odot}$ (e.g., our ‘He02r’ model). However, about 1000 d after the explosion, the luminosities of our surviving companion models are still significantly increasing for a few ten years as the companions expand, and they will reach the maximum luminosity ($\gtrsim 4000 L_{\odot}$) at about 10^4 d. This means that a detectable rebrightening of the light-curve of SN 2011fe would be seen at a later epoch if there were a shocked He-star companion with a mass of $\lesssim 0.95 M_{\odot}$. Based on our comparison with current late-time observations of SN 2011fe, He-star companions with masses above $0.95 M_{\odot}$ are ruled out. We strongly encourage future observations to test this hypothesis, which will help complete the picture of constraints on the He-star as a companion to the progenitor of SN 2011fe.

We did not consider the rotation of an accreting WD when constructing the companion star model at the moment of SN explosion in our 1D binary evolution calculation (Liu et al. 2013b). The accretion from the companion star is expected to spin up the WD, delaying its explosion (i.e., the ‘spin up/spin down’ model; Justham 2011; Di Stefano et al. 2011). If the spin-down timescale is long enough, the He-star companion in this model could have evolved to a WD at the moment of SN explosion. In this case, the post-impact properties of the surviving companion star would be different from the results in this work because of a much weaker ejecta–companion interaction. This may lead to a dim surviving companion star that could explain the extreme late-time light-curve of SN 2011fe. However, the exact spin-down timescale of the WD in the ‘spin up/spin down’ model is quite unknown.

5. SUMMARY AND CONCLUSION

In this work, we map the computed surviving He-star companion models from our previous 3D hydrodynamical simulations of ejecta-companion interaction (Liu et al. 2013b) into the 1D stellar evolution code MESA (Paxton et al. 2011, 2018) to follow their subsequent re-equilibration evolution. The main goal of this work is to determine the expected observable signatures of surviving He-star companions of SNe Ia, which can be instrumental in searches for such objects in historical SN Ia remnants. Our main results and conclusions can be summarized as follows:

- (1) We find that the He-star companions are strongly heated and inflated during the ejecta–companion interaction. They continue to expand for a few

tens of years before they start to contract. As a consequence, they become significantly overluminous over a Kelvin–Helmholtz timescale after the impact. After re-establishing thermal equilibrium, the stars continue to evolve on a track very close to that of an unperturbed He star with the same mass.

- (2) Our ‘He01’ and ‘He02’ models absorb energies of $E_{\text{in}} \sim 1.68 \times 10^{49}$ erg and 1.19×10^{49} erg during the ejecta–companion interaction. During the thermal re-equilibration phase, they reach a peak luminosity of $L_{\text{peak}} \sim 16000 L_{\odot}$ and $5800 L_{\odot}$ at about $t_{\text{peak}} \sim 15$ yr and 30 yr, respectively.
- (3) The luminosities of our surviving He-star companions become comparable to those of a normal He-star that has not been impacted and heated a few hundred years after the explosion. This suggests that the identification of surviving He-star companions is more promising in the young nearby SNRs (younger than a few 100 yr).
- (4) We find that an inclusion of the orbital motion and the spin of the He-star companion into the impact simulation does not play an important role in determining the properties of surviving He-star companions (Figs 2 and 3). For example, the ‘He01r’ model takes $t_{\text{peak}} \sim 22$ yr to reach its peak luminosity of $L_{\text{peak}} \sim 15000 L_{\odot}$, and the two orbital parameters (t_{peak} and L_{peak}) are prolonged t_{peak} by a factor of 1.5 and lower L_{peak} by 1.1 compared with model ‘He01’ model.
- (5) Artificially adjusting the kinetic energy of the SN ejecta by scaling the velocities of the original ‘W7 explosion model’ in our impact simulations, we find that the surviving He-star companion takes a longer time to reach a lower peak luminosity during the thermal re-equilibration phase in the case with a higher kinetic energy. For a given He-star companion model ‘He01r’, we find that the post-impact peak luminosity L_{peak} of the star decreases by a factor of about 1.4, and the time of peak luminosity t_{peak} increases by a factor of about 5, as the kinetic energy of SN Ia ejecta increases from 0.8×10^{51} erg to 1.6×10^{51} erg (Fig. 4).
- (6) The surface rotational speeds of companions in model He01r and He02r significantly decrease after the impact due to the angular momentum loss and their expansion. About 20–30 yr after the impact, they drop to around 30–40 km s^{−1} (i.e., 12%–%13 of the original value) when the stars expand

to the maximum size. The star then shrinks and its surface rotational speed increases again. After thermal equilibrium is reestablished, it becomes a fast-rotating object again. We suggest that the surviving He-star companions of SNe Ia could rotate slowly although they are fast-rotating stars originally, which depends on the ages of SNRs.

- (7) Comparing our results with the late-time light curve of the best observed SN Ia, SN 2011fe, we find that the predicted luminosities of the surviving He-star companions are generally higher significantly than the observed luminosity of SN 2011fe about 1000 d after the impact. This conflict seems to rule out the existence of a shocked surviving He-star companion in nearby SN 2011fe.
- (8) Our results suggest that the surviving He-star companion should begin to dominate the SN Ia late-time light-curve about 1000 days after maximum light.
- (9) Based on our results, there is a slight chance that current late-time light curve observations of SN 2011fe still miss a contribution from the shock-heated He-star companion that would have a mass of $\lesssim 0.95 M_{\odot}$. In this case, however, our models suggest that a rebrightening of the light-curve of SN 2011fe will be seen soon. We encourage future observations to test this hypothesis and to place further constraints on a He-star as potential companion in the progenitor system of SN 2011fe.

1 We thank the anonymous referee for constructive
 2 comments that helped to improve this paper. ZWL
 3 is supported by the National Key R&D Program of
 4 China (No. 2021YFA1600401), the National Natural
 5 Science Foundation of China (NSFC, No. 11873016),
 6 the Chinese Academy of Sciences (CAS) and the Nat-
 7 ural Science Foundation of Yunnan Province (No.
 8 202001AW070007). The work of FR is supported by
 9 the Klaus Tschira Foundation and by the Deutsche
 10 Forschungsgemeinschaft (DFG, German Research Foun-
 11 dation) – Project-ID 138713538 – SFB 881 (“The Milky
 12 Way System”, Subproject A10). The authors gratefully
 13 acknowledge the ‘PHOENIX Supercomputing Platform’
 14 jointly operated by the Binary Population Synthesis
 15 Group and the Stellar Astrophysics Group at Yunnan
 16 Observatories, CAS.

Software: STELLAR GADGET (Springel et al. 2001; Springel 2005; Pakmor et al. 2012), MESA (Paxton et al. 2011, 2013, 2015, 2018), matplotlib (Hunter 2007).

REFERENCES

- Bauer, E. B., White, C. J., & Bildsten, L. 2019, *ApJ*, 887, 68, doi: [10.3847/1538-4357/ab4ea4](https://doi.org/10.3847/1538-4357/ab4ea4)
- Bedin, L. R., Ruiz-Lapuente, P., González Hernández, J. I., et al. 2014, *MNRAS*, 439, 354, doi: [10.1093/mnras/stt2460](https://doi.org/10.1093/mnras/stt2460)
- Benz, W., Hills, J. G., & Thielemann, F. K. 1989, *ApJ*, 342, 986, doi: [10.1086/167656](https://doi.org/10.1086/167656)
- Bloom, J. S., Kasen, D., Shen, K. J., et al. 2012, *ApJL*, 744, L17, doi: [10.1088/2041-8205/744/2/L17](https://doi.org/10.1088/2041-8205/744/2/L17)
- Boehner, P., Plewa, T., & Langer, N. 2017, *MNRAS*, 465, 2060, doi: [10.1093/mnras/stw2737](https://doi.org/10.1093/mnras/stw2737)
- Brown, P. J., Dawson, K. S., de Pasquale, M., et al. 2012, *ApJ*, 753, 22, doi: [10.1088/0004-637X/753/1/22](https://doi.org/10.1088/0004-637X/753/1/22)
- Chomiuk, L., Soderberg, A. M., Moe, M., et al. 2012, *ApJ*, 750, 164, doi: [10.1088/0004-637X/750/2/164](https://doi.org/10.1088/0004-637X/750/2/164)
- Dan, M., Rosswog, S., Guillochon, J., & Ramirez-Ruiz, E. 2011, *ApJ*, 737, 89, doi: [10.1088/0004-637X/737/2/89](https://doi.org/10.1088/0004-637X/737/2/89)
- Di Stefano, R., Voss, R., & Claeys, J. S. W. 2011, *ApJL*, 738, L1, doi: [10.1088/2041-8205/738/1/L1](https://doi.org/10.1088/2041-8205/738/1/L1)
- Dimitriadis, G., Sullivan, M., Kerzendorf, W., et al. 2017, *MNRAS*, 468, 3798, doi: [10.1093/mnras/stx683](https://doi.org/10.1093/mnras/stx683)
- Edwards, Z. I., Pagnotta, A., & Schaefer, B. E. 2012, *ApJL*, 747, L19, doi: [10.1088/2041-8205/747/2/L19](https://doi.org/10.1088/2041-8205/747/2/L19)
- Fink, M., Hillebrandt, W., & Röpke, F. K. 2007, *A&A*, 476, 1133, doi: [10.1051/0004-6361:20078438](https://doi.org/10.1051/0004-6361:20078438)
- Fink, M., Kromer, M., Seitzzahl, I. R., et al. 2014, *MNRAS*, 438, 1762, doi: [10.1093/mnras/stt2315](https://doi.org/10.1093/mnras/stt2315)
- Foley, R. J., McCully, C., Jha, S. W., et al. 2014, *ApJ*, 792, 29, doi: [10.1088/0004-637X/792/1/29](https://doi.org/10.1088/0004-637X/792/1/29)
- Foley, R. J., Challis, P. J., Chornock, R., et al. 2013, *ApJ*, 767, 57, doi: [10.1088/0004-637X/767/1/57](https://doi.org/10.1088/0004-637X/767/1/57)
- Fuhrmann, K. 2005, *MNRAS*, 359, L35, doi: [10.1111/j.1745-3933.2005.00032.x](https://doi.org/10.1111/j.1745-3933.2005.00032.x)
- Gaia Collaboration, Prusti, T., de Bruijne, J. H. J., et al. 2016, *A&A*, 595, A1, doi: [10.1051/0004-6361/201629272](https://doi.org/10.1051/0004-6361/201629272)
- Gaia Collaboration, Brown, A. G. A., Vallenari, A., et al. 2018, *A&A*, 616, A1, doi: [10.1051/0004-6361/201833051](https://doi.org/10.1051/0004-6361/201833051)
- González Hernández, J. I., Ruiz-Lapuente, P., Filippenko, A. V., et al. 2009, *ApJ*, 691, 1, doi: [10.1088/0004-637X/691/1/1](https://doi.org/10.1088/0004-637X/691/1/1)
- González Hernández, J. I., Ruiz-Lapuente, P., Tabernero, H. M., et al. 2012, *Nature*, 489, 533, doi: [10.1038/nature11447](https://doi.org/10.1038/nature11447)
- Graham, M. L., Nugent, P. E., Sullivan, M., et al. 2015, *MNRAS*, 454, 1948, doi: [10.1093/mnras/stv1888](https://doi.org/10.1093/mnras/stv1888)
- Gronow, S., Collins, C., Ohlmann, S. T., et al. 2020, *A&A*, 635, A169, doi: [10.1051/0004-6361/201936494](https://doi.org/10.1051/0004-6361/201936494)
- Gronow, S., Collins, C. E., Sim, S. A., & Roepke, F. K. 2021, arXiv e-prints, arXiv:2102.06719, <https://arxiv.org/abs/2102.06719>
- Hachisu, I., Kato, M., & Nomoto, K. 1996, *ApJL*, 470, L97, doi: [10.1086/310303](https://doi.org/10.1086/310303)
- Han, Z. 2008, *ApJL*, 677, L109, doi: [10.1086/588191](https://doi.org/10.1086/588191)
- Han, Z., & Podsiadlowski, P. 2004, *MNRAS*, 350, 1301, doi: [10.1111/j.1365-2966.2004.07713.x](https://doi.org/10.1111/j.1365-2966.2004.07713.x)
- Heger, A., & Woosley, S. E. 2010, *ApJ*, 724, 341, doi: [10.1088/0004-637X/724/1/341](https://doi.org/10.1088/0004-637X/724/1/341)
- Hillebrandt, W., Kromer, M., Röpke, F. K., & Ruiter, A. J. 2013, *Frontiers of Physics*, 8, 116, doi: [10.1007/s11467-013-0303-2](https://doi.org/10.1007/s11467-013-0303-2)
- Horesh, A., Kulkarni, S. R., Fox, D. B., et al. 2012, *ApJ*, 746, 21, doi: [10.1088/0004-637X/746/1/21](https://doi.org/10.1088/0004-637X/746/1/21)
- Hoyle, F., & Fowler, W. A. 1960, *ApJ*, 132, 565, doi: [10.1086/146963](https://doi.org/10.1086/146963)
- Hunter, J. D. 2007, *Computing in Science & Engineering*, 9, 90, doi: [10.1109/MCSE.2007.55](https://doi.org/10.1109/MCSE.2007.55)
- Iben, Jr., I., & Tutukov, A. V. 1984, *ApJ*, 284, 719, doi: [10.1086/162455](https://doi.org/10.1086/162455)
- Ihara, Y., Ozaki, J., Doi, M., et al. 2007, *PASJ*, 59, 811, doi: [10.1093/pasj/59.4.811](https://doi.org/10.1093/pasj/59.4.811)

- Ilkov, M., & Soker, N. 2012, *MNRAS*, 419, 1695, doi: [10.1111/j.1365-2966.2011.19833.x](https://doi.org/10.1111/j.1365-2966.2011.19833.x)
- Jordan, IV, G. C., Perets, H. B., Fisher, R. T., & van Rossum, D. R. 2012, *ApJL*, 761, L23, doi: [10.1088/2041-8205/761/2/L23](https://doi.org/10.1088/2041-8205/761/2/L23)
- Justham, S. 2011, *ApJL*, 730, L34+, doi: [10.1088/2041-8205/730/2/L34](https://doi.org/10.1088/2041-8205/730/2/L34)
- Kelly, P. L., Fox, O. D., Filippenko, A. V., et al. 2014, *ApJ*, 790, 3, doi: [10.1088/0004-637X/790/1/3](https://doi.org/10.1088/0004-637X/790/1/3)
- Kerzendorf, W. E., Childress, M., Scharwächter, J., Do, T., & Schmidt, B. P. 2014, *ApJ*, 782, 27, doi: [10.1088/0004-637X/782/1/27](https://doi.org/10.1088/0004-637X/782/1/27)
- Kerzendorf, W. E., Long, K. S., Winkler, P. F., & Do, T. 2018a, *MNRAS*, 479, 5696, doi: [10.1093/mnras/sty1863](https://doi.org/10.1093/mnras/sty1863)
- Kerzendorf, W. E., Schmidt, B. P., Asplund, M., et al. 2009, *ApJ*, 701, 1665, doi: [10.1088/0004-637X/701/2/1665](https://doi.org/10.1088/0004-637X/701/2/1665)
- Kerzendorf, W. E., Schmidt, B. P., Laird, J. B., Podsiadlowski, P., & Bessell, M. S. 2012, *ApJ*, 759, 7, doi: [10.1088/0004-637X/759/1/7](https://doi.org/10.1088/0004-637X/759/1/7)
- Kerzendorf, W. E., Strampelli, G., Shen, K. J., et al. 2018b, *MNRAS*, 479, 192, doi: [10.1093/mnras/sty1357](https://doi.org/10.1093/mnras/sty1357)
- Kerzendorf, W. E., Yong, D., Schmidt, B. P., et al. 2013, *ApJ*, 774, 99, doi: [10.1088/0004-637X/774/2/99](https://doi.org/10.1088/0004-637X/774/2/99)
- Kerzendorf, W. E., McCully, C., Taubenberger, S., et al. 2017, *MNRAS*, 472, 2534, doi: [10.1093/mnras/stx1923](https://doi.org/10.1093/mnras/stx1923)
- Kromer, M., Fink, M., Stanishev, V., et al. 2013, *MNRAS*, 429, 2287, doi: [10.1093/mnras/sts498](https://doi.org/10.1093/mnras/sts498)
- Kushnir, D., Katz, B., Dong, S., Livne, E., & Fernández, R. 2013, *ApJL*, 778, L37, doi: [10.1088/2041-8205/778/2/L37](https://doi.org/10.1088/2041-8205/778/2/L37)
- Lach, F., Callan, F. P., Bubeck, D., et al. 2021a, arXiv e-prints, arXiv:2109.02926. <https://arxiv.org/abs/2109.02926>
- Lach, F., Callan, F. P., Sim, S. A., & Roepke, F. K. 2021b, arXiv e-prints, arXiv:2111.14394. <https://arxiv.org/abs/2111.14394>
- Li, C.-J., Chu, Y.-H., Gruendl, R. A., et al. 2017, *ApJ*, 836, 85, doi: [10.3847/1538-4357/836/1/85](https://doi.org/10.3847/1538-4357/836/1/85)
- Li, C.-J., Kerzendorf, W. E., Chu, Y.-H., et al. 2019, *ApJ*, 886, 99, doi: [10.3847/1538-4357/ab4a03](https://doi.org/10.3847/1538-4357/ab4a03)
- Li, W., Bloom, J. S., Podsiadlowski, P., et al. 2011, *Nature*, 480, 348, doi: [10.1038/nature10646](https://doi.org/10.1038/nature10646)
- Litke, K. C., Chu, Y.-H., Holmes, A., et al. 2017, *ApJ*, 837, 111, doi: [10.3847/1538-4357/aa5d57](https://doi.org/10.3847/1538-4357/aa5d57)
- Liu, Z., & Stancliffe, R. J. 2020, *A&A*, 641, A20, doi: [10.1051/0004-6361/202038443](https://doi.org/10.1051/0004-6361/202038443)
- Liu, Z.-W., Kromer, M., Fink, M., et al. 2013a, *ApJ*, 778, 121, doi: [10.1088/0004-637X/778/2/121](https://doi.org/10.1088/0004-637X/778/2/121)
- Liu, Z.-W., Pakmor, R., Röpke, F. K., et al. 2013b, *A&A*, 554, A109, doi: [10.1051/0004-6361/201220903](https://doi.org/10.1051/0004-6361/201220903)
- Liu, Z. W., Pakmor, R., Röpke, F. K., et al. 2012, *A&A*, 548, A2, doi: [10.1051/0004-6361/201219357](https://doi.org/10.1051/0004-6361/201219357)
- Liu, Z.-W., Röpke, F. K., Zeng, Y., & Heger, A. 2021, *A&A*, 654, A103, doi: [10.1051/0004-6361/202141518](https://doi.org/10.1051/0004-6361/202141518)
- Liu, Z.-W., & Stancliffe, R. J. 2018, *MNRAS*, 475, 5257, doi: [10.1093/mnras/sty172](https://doi.org/10.1093/mnras/sty172)
- Liu, Z.-W., Stancliffe, R. J., Abate, C., & Wang, B. 2015, *ApJ*, 808, 138, doi: [10.1088/0004-637X/808/2/138](https://doi.org/10.1088/0004-637X/808/2/138)
- Liu, Z.-W., & Zeng, Y. 2021, *MNRAS*, 500, 301, doi: [10.1093/mnras/staa3280](https://doi.org/10.1093/mnras/staa3280)
- Liu, Z.-W., Pakmor, R., Seitzzahl, I. R., et al. 2013c, *ApJ*, 774, 37, doi: [10.1088/0004-637X/774/1/37](https://doi.org/10.1088/0004-637X/774/1/37)
- Livio, M., & Riess, A. G. 2003, *ApJL*, 594, L93, doi: [10.1086/378765](https://doi.org/10.1086/378765)
- Lundqvist, P., Nyholm, A., Taddia, F., et al. 2015, *A&A*, 577, A39, doi: [10.1051/0004-6361/201525719](https://doi.org/10.1051/0004-6361/201525719)
- Maoz, D., & Mannucci, F. 2008, *MNRAS*, 388, 421, doi: [10.1111/j.1365-2966.2008.13403.x](https://doi.org/10.1111/j.1365-2966.2008.13403.x)
- Maoz, D., Mannucci, F., & Nelemans, G. 2014, *ARA&A*, 52, 107, doi: [10.1146/annurev-astro-082812-141031](https://doi.org/10.1146/annurev-astro-082812-141031)
- Margutti, R., Soderberg, A. M., Chomiuk, L., et al. 2012, *ApJ*, 751, 134, doi: [10.1088/0004-637X/751/2/134](https://doi.org/10.1088/0004-637X/751/2/134)
- Marietta, E., Burrows, A., & Fryxell, B. 2000, *ApJS*, 128, 615, doi: [10.1086/313392](https://doi.org/10.1086/313392)
- McCully, C., Jha, S. W., Foley, R. J., et al. 2014, *Nature*, 512, 54, doi: [10.1038/nature13615](https://doi.org/10.1038/nature13615)
- McCully, C., Jha, S. W., Scalzo, R. A., et al. 2021, arXiv e-prints, arXiv:2106.04602. <https://arxiv.org/abs/2106.04602>
- Nomoto, K. 1982, *ApJ*, 253, 798, doi: [10.1086/159682](https://doi.org/10.1086/159682)
- Nomoto, K., Thielemann, F.-K., & Yokoi, K. 1984, *ApJ*, 286, 644, doi: [10.1086/162639](https://doi.org/10.1086/162639)
- Nugent, P. E., Sullivan, M., Cenko, S. B., et al. 2011, *Nature*, 480, 344, doi: [10.1038/nature10644](https://doi.org/10.1038/nature10644)
- Pagnotta, A., & Schaefer, B. E. 2015, *ApJ*, 799, 101, doi: [10.1088/0004-637X/799/1/101](https://doi.org/10.1088/0004-637X/799/1/101)
- Pagnotta, A., Walker, E. S., & Schaefer, B. E. 2014, *ApJ*, 788, 173, doi: [10.1088/0004-637X/788/2/173](https://doi.org/10.1088/0004-637X/788/2/173)
- Pakmor, R., Edelmann, P., Röpke, F. K., & Hillebrandt, W. 2012, *MNRAS*, 424, 2222, doi: [10.1111/j.1365-2966.2012.21383.x](https://doi.org/10.1111/j.1365-2966.2012.21383.x)
- Pakmor, R., Kromer, M., Röpke, F. K., et al. 2010, *Nature*, 463, 61, doi: [10.1038/nature08642](https://doi.org/10.1038/nature08642)
- Pakmor, R., Röpke, F. K., Weiss, A., & Hillebrandt, W. 2008, *A&A*, 489, 943, doi: [10.1051/0004-6361:200810456](https://doi.org/10.1051/0004-6361:200810456)
- Pan, K.-C., Ricker, P. M., & Taam, R. E. 2012a, *ApJ*, 750, 151, doi: [10.1088/0004-637X/750/2/151](https://doi.org/10.1088/0004-637X/750/2/151)
- . 2012b, *ApJ*, 760, 21, doi: [10.1088/0004-637X/760/1/21](https://doi.org/10.1088/0004-637X/760/1/21)
- . 2013, *ApJ*, 773, 49, doi: [10.1088/0004-637X/773/1/49](https://doi.org/10.1088/0004-637X/773/1/49)

- Paxton, B., Bildsten, L., Dotter, A., et al. 2011, *ApJS*, 192, 3, doi: [10.1088/0067-0049/192/1/3](https://doi.org/10.1088/0067-0049/192/1/3)
- Paxton, B., Cantiello, M., Arras, P., et al. 2013, *ApJS*, 208, 4, doi: [10.1088/0067-0049/208/1/4](https://doi.org/10.1088/0067-0049/208/1/4)
- Paxton, B., Marchant, P., Schwab, J., et al. 2015, *ApJS*, 220, 15, doi: [10.1088/0067-0049/220/1/15](https://doi.org/10.1088/0067-0049/220/1/15)
- Paxton, B., Schwab, J., Bauer, E. B., et al. 2018, *ApJS*, 234, 34, doi: [10.3847/1538-4365/aaa5a8](https://doi.org/10.3847/1538-4365/aaa5a8)
- Perlmutter, S., Aldering, G., Goldhaber, G., et al. 1999, *ApJ*, 517, 565, doi: [10.1086/307221](https://doi.org/10.1086/307221)
- Phillips, M. M. 1993, *ApJL*, 413, L105, doi: [10.1086/186970](https://doi.org/10.1086/186970)
- Phillips, M. M., Lira, P., Suntzeff, N. B., et al. 1999, *AJ*, 118, 1766, doi: [10.1086/301032](https://doi.org/10.1086/301032)
- Podsiadlowski, P. 2003, arXiv e-prints, astro. <https://arxiv.org/abs/astro-ph/0303660>
- Rauscher, T., Heger, A., Hoffman, R. D., & Woosley, S. E. 2002, *ApJ*, 576, 323, doi: [10.1086/341728](https://doi.org/10.1086/341728)
- Riess, A. G., Filippenko, A. V., Challis, P., et al. 1998, *AJ*, 116, 1009, doi: [10.1086/300499](https://doi.org/10.1086/300499)
- Röpke, F. K., Hillebrandt, W., Schmidt, W., et al. 2007, *ApJ*, 668, 1132, doi: [10.1086/521347](https://doi.org/10.1086/521347)
- Röpke, F. K., & Niemeyer, J. C. 2007, *A&A*, 464, 683, doi: [10.1051/0004-6361:20066585](https://doi.org/10.1051/0004-6361:20066585)
- Röpke, F. K., Kromer, M., Seitenzahl, I. R., et al. 2012, *ApJL*, 750, L19, doi: [10.1088/2041-8205/750/1/L19](https://doi.org/10.1088/2041-8205/750/1/L19)
- Rosswog, S., Kasen, D., Guillochon, J., & Ramirez-Ruiz, E. 2009, *ApJL*, 705, L128, doi: [10.1088/0004-637X/705/2/L128](https://doi.org/10.1088/0004-637X/705/2/L128)
- Ruiz-Lapuente, P. 2019, *NewAR*, 85, 101523, doi: [10.1016/j.newar.2019.101523](https://doi.org/10.1016/j.newar.2019.101523)
- Ruiz-Lapuente, P., Damiani, F., Bedin, L., et al. 2018, *ApJ*, 862, 124, doi: [10.3847/1538-4357/aac9c4](https://doi.org/10.3847/1538-4357/aac9c4)
- Ruiz-Lapuente, P., Comeron, F., Méndez, J., et al. 2004, *Nature*, 431, 1069, doi: [10.1038/nature03006](https://doi.org/10.1038/nature03006)
- Schaefer, B. E., & Pagnotta, A. 2012, *Nature*, 481, 164, doi: [10.1038/nature10692](https://doi.org/10.1038/nature10692)
- Schmidt, B. P., Suntzeff, N. B., Phillips, M. M., et al. 1998, *ApJ*, 507, 46, doi: [10.1086/306308](https://doi.org/10.1086/306308)
- Seitenzahl, I. R., Ciaraldi-Schoolmann, F., Röpke, F. K., et al. 2013, *MNRAS*, 429, 1156, doi: [10.1093/mnras/sts402](https://doi.org/10.1093/mnras/sts402)
- Shappee, B. J., Kochanek, C. S., & Stanek, K. Z. 2013, *ApJ*, 765, 150, doi: [10.1088/0004-637X/765/2/150](https://doi.org/10.1088/0004-637X/765/2/150)
- Shappee, B. J., & Stanek, K. Z. 2011, *ApJ*, 733, 124, doi: [10.1088/0004-637X/733/2/124](https://doi.org/10.1088/0004-637X/733/2/124)
- Shappee, B. J., Stanek, K. Z., Kochanek, C. S., & Garnavich, P. M. 2017, *ApJ*, 841, 48, doi: [10.3847/1538-4357/aa6eab](https://doi.org/10.3847/1538-4357/aa6eab)
- Shen, K. J., & Bildsten, L. 2007, *ApJ*, 660, 1444, doi: [10.1086/513457](https://doi.org/10.1086/513457)
- Shen, K. J., Boubert, D., Gänsicke, B. T., et al. 2018, *ApJ*, 865, 15, doi: [10.3847/1538-4357/aad55b](https://doi.org/10.3847/1538-4357/aad55b)
- Sim, S. A., Röpke, F. K., Hillebrandt, W., et al. 2010, *ApJL*, 714, L52, doi: [10.1088/2041-8205/714/1/L52](https://doi.org/10.1088/2041-8205/714/1/L52)
- Soker, N. 2019, *NewAR*, 87, 101535, doi: [10.1016/j.newar.2020.101535](https://doi.org/10.1016/j.newar.2020.101535)
- Springel, V. 2005, *MNRAS*, 364, 1105, doi: [10.1111/j.1365-2966.2005.09655.x](https://doi.org/10.1111/j.1365-2966.2005.09655.x)
- Springel, V., Yoshida, N., & White, S. D. M. 2001, *NewA*, 6, 79, doi: [10.1016/S1384-1076\(01\)00042-2](https://doi.org/10.1016/S1384-1076(01)00042-2)
- Townsley, D. M., Miles, B. J., Shen, K. J., & Kasen, D. 2019, *ApJL*, 878, L38, doi: [10.3847/2041-8213/ab27cd](https://doi.org/10.3847/2041-8213/ab27cd)
- Tucker, M. A., Ashall, C., Shappee, B. J., et al. 2021a, arXiv e-prints, arXiv:2111.00016, <https://arxiv.org/abs/2111.00016>
- Tucker, M. A., Shappee, B. J., Kochanek, C. S., et al. 2021b, arXiv e-prints, arXiv:2111.01144, <https://arxiv.org/abs/2111.01144>
- Wang, B., Chen, X., Meng, X., & Han, Z. 2009, *ApJ*, 701, 1540, doi: [10.1088/0004-637X/701/2/1540](https://doi.org/10.1088/0004-637X/701/2/1540)
- Weaver, T. A., Zimmerman, G. B., & Woosley, S. E. 1978, *ApJ*, 225, 1021, doi: [10.1086/156569](https://doi.org/10.1086/156569)
- Webbink, R. F. 1984, *ApJ*, 277, 355, doi: [10.1086/161701](https://doi.org/10.1086/161701)
- Wheeler, J. C., Lecar, M., & McKee, C. F. 1975, *ApJ*, 200, 145, doi: [10.1086/153771](https://doi.org/10.1086/153771)
- Whelan, J., & Iben, Jr., I. 1973, *ApJ*, 186, 1007, doi: [10.1086/152565](https://doi.org/10.1086/152565)
- Woosley, S. E., Heger, A., & Weaver, T. A. 2002, *Reviews of Modern Physics*, 74, 1015, doi: [10.1103/RevModPhys.74.1015](https://doi.org/10.1103/RevModPhys.74.1015)
- Woosley, S. E., Taam, R. E., & Weaver, T. A. 1986, *ApJ*, 301, 601, doi: [10.1086/163926](https://doi.org/10.1086/163926)
- Zeng, Y., Liu, Z.-W., & Han, Z. 2020, *ApJ*, 898, 12, doi: [10.3847/1538-4357/ab9943](https://doi.org/10.3847/1538-4357/ab9943)